649



# Atom-optical properties of a standing-wave light field

J. J. McClelland

*Electron Physics Group, National Institute of Standards and Technology, Gaithersburg, Maryland 20899*

Received November 14, 1994; revised manuscript received March 2, 1995

The focusing of atoms to nanometer-scale dimensions by a near-resonant standing-wave light field is examined from a particle optics perspective. The classical equation of motion for atoms traveling through the lens formed by a node of the standing wave is derived and converted to a spatial trajectory equation. A paraxial solution is obtained, which results in simple expressions for the focal properties of the lens, useful for estimating its behavior. Aberrations are also discussed, and an exact numerical solution of the trajectory equation is presented. The effects on focal linewidth of angular collimation and velocity spread in the atomic beam are investigated, and it is shown that angular collimation has a much more significant effect than velocity spread, even when the velocity spread is thermal.

## 1. INTRODUCTION

The focusing of neutral atoms by use of near-resonant light fields has been the subject of intense interest lately. This interest has been driven to a large extent by the possibility of generating focal spots on the nanometer scale by use of specially configured laser intensity profiles. Of particular interest has been the combination of high-resolution focusing with atomic deposition onto a substrate. The result is a technique for nanostructure fabrication with possibilities for both high resolution and massive parallelism.

The first proposal of nanometer-scale focusing was made by Balykin and Letokhov,[1] who suggested the possibility of deep focusing by using the bore of a focused $TEM_{01}^*$ (donut-mode) laser beam as a lens for atoms. A wave-mechanical analysis of this configuration was done by Gallatin and Gould,[2] and a particle optics approach was presented by McClelland and Scheinfein.[3] The particle optics approach, in which the atom lens formed by the laser light was treated as an optical element analogous to a charged-particle magnetic lens, proved useful for predicting the first-order properties and also the aberrations of the lens. A useful discussion of the correspondence between particle and wave approaches to atom optics can be found in the review article by Adams *et al.*[4]

Experimentally, focusing atoms inside a $TEM_{01}^*$ laser beam is not readily accomplished. On the other hand, several experiments have been performed in which atoms are focused by traversing a standing-wave laser field. In this configuration, each node of the standing wave acts as an individual lens, and the entire standing wave acts as a lens array. Sleator *et al.*[5] showed that metastable He atoms could be focused in a single period of a large-period standing wave, and they observed actual imaging of an object. Timp *et al.*[6] used a standing light wave to focus Na atoms as they deposited onto a substrate. In a similar experiment, McClelland *et al.*[7] focused Cr atoms onto a substrate by using a standing wave, creating permanent nanostructures that could be observed with a range of microscopy techniques.

As demonstrated by the experiments of Timp *et al.*[6] and McClelland *et al.*,[7] there are several advantages to using a standing wave for focused atomic deposition. Because a standing-wave light field repeats with a periodicity of order $\lambda/2$, where $\lambda$ is the wavelength of the light, a large array of structures can be fabricated in parallel. In addition, the individual lenses in the lens array formed by the standing wave have a size of order $\lambda/2$. Starting with this small lens size (typically 200–300 nm for visible light), it is easier to achieve focusing on the nanometer scale.

It is the purpose of this paper to apply the particle optics approach used by McClelland and Scheinfein[3] to the analysis of atom focusing in a standing wave. Berggren *et al.*[8] presented a time-dependent trajectory analysis of this problem and were able to derive some properties of the lens formed in a node of the standing wave. In the present study, time is eliminated from the equation of motion, and a paraxial equation is derived. Solution of the paraxial equation provides a simple framework for characterizing the basic behavior of the atomic lens formed by each node of the standing wave in terms of a single excitation parameter. Aberrations are also discussed, and in the last section an exact numerical solution is presented that does not rely on the paraxial approximation.

## 2. LIGHT FORCE ON AN ATOM

The light force on an atom has been studied rather extensively, and a relatively thorough understanding, at least for a two-level atom, has evolved based on a dressed-state treatment.[9] In general, the force felt by an atom in a light field has both velocity-dependent and conservative terms. The velocity-dependent terms, which arise from Doppler shifts experienced by the atom and from nonadiabatic effects, have been utilized extensively for laser cooling.[10] Many practical applications have made use of these dissipative terms, such as the slowing and trapping of atoms and the collimation of atom beams to a high degree. However, the velocity-dependent terms must be negligible if a particle optics approach to laser focusing of atoms is to be applicable in a straightforward way. Many of the fundamental concepts in particle optics presume a conservative potential.

Fortunately, for a wide range of parameters the velocity-dependent terms in the light force can be ignored, and a conservative potential can be derived. In this regime the light force is often referred to as the dipole force, since it can be thought of classically as the interaction of the induced atomic dipole with a gradient in the electric field of the laser. If the laser intensity is relatively low and/or the detuning from resonance is relatively large, such that there is not a significant population of excited-state atoms, the light force potential on a two-level atom can be written as[9]

$$U(x, y, z) = \frac{\hbar\gamma^2}{8\Delta} \frac{I(x, y, z)}{I_s}, \tag{1}$$

where $\gamma$ is the natural linewidth of the atomic transition (in radians per second), $\Delta$ is the detuning of the laser frequency from the atomic resonance (also in radians per second), $I(x, y, z)$ is the laser intensity, and $I_s$ is the saturation intensity associated with the atomic transition. $U(x, y, z)$ is sometimes expressed in terms of the Rabi frequency $\Omega(x, y, z) = \gamma[I(x, y, z)/2I_s]^{1/2}$ as $U(x, y, z) = \hbar\Omega(x, y, z)^2/4\Delta$. We note that Eq. (1) is strictly valid only for a two-level atom. It can, however, be used for more complicated atoms, such as those with multiple magnetic sublevels, provided that optical pumping and coherences can be ignored.

If one is willing to accept some restrictions on the range of validity, Eq. (1) can be generalized to include the effects of saturation, which occurs for higher laser intensity and/or smaller detunings. The key assumptions are (1) that the atom moves slowly enough in the spatially varying laser field so that equilibrium between the internal state and the radiation field is always maintained (i.e., adiabatic conditions) and (2) that the atom does not spend long enough in the field to experience enough spontaneous emission to modify significantly its trajectory. The time scale over which both spontaneous emission and the return to equilibrium occur is $1/\gamma$, so condition (1) is obtained if $(v_z/I)(dI/dz) \ll \gamma$, and condition (2) is obtained if $(L/v_z) \gg \gamma^{-1}$, where $v_z$ is the characteristic velocity in the $\hat{z}$ direction and $L$ is the characteristic length over which the interaction occurs. In this regime the potential is[11]

$$U(x, y, z) = \frac{\hbar\Delta}{2} \ln[1 + p(x, y, z)], \tag{2}$$

where

$$p(x, y, z) = \frac{I(x, y, z)}{I_s} \frac{\gamma^2}{\gamma^2 + 4\Delta^2} \tag{3}$$

$$= p_0 G(x, y, z). \tag{4}$$

In Eq. (4) the spatial dependence of $p(x, y, z)$ is grouped into a dimensionless function $G(x, y, z)$, and the laser parameter dependence is grouped into the quantity

$$p_0 = \frac{I_0}{I_s} \frac{\gamma^2}{\gamma^2 + 4\Delta^2}, \tag{5}$$

where $I_0$ is the laser intensity at that point in space where $G(x, y, z) = 1$. We observe that, for large detuning and/or small intensity, Eq. (2) reduces to the simpler Eq. (1). For the calculations in this paper we choose Eq. (2) as a starting point, since it can treat higher-intensity/smaller-detuning situations, albeit in an approximate manner. One should bear in mind that, if $p(x, y, z)$ is substantially greater than 1, calculations based on the results to be derived below are valid only in an adiabatic limit, and, conversely, if $p(x, y, z) < 1$, the results should be fairly accurate.

## 3. EQUATION OF MOTION

We now consider the equation of motion of an atom traveling through a standing-wave laser field. The spatial dependence $G(x, y, z)$ of the laser light intensity for a laser beam propagating along $\hat{x}$ can be written as a product of a standing wave in $x$ and an envelope function $g(z)$ in $z$ (see Fig. 1):

$$G(x, y, z) = g(z)\sin^2 kx, \tag{6}$$

where $k = 2\pi/\lambda$ is the wave vector of the laser light and $g(z)$ is the profile of the laser beam along $\hat{z}$ (for instance, a Gaussian). We have ignored any $y$ dependence of the laser intensity because it is assumed that any light forces along this direction will be negligible compared with those resulting from the standing wave. We thus assume that there is translational symmetry along the $y$ axis, so this dimension can be ignored, and the problem reduces to a two-dimensional one with motion determined by the equations

$$\ddot{x} + \frac{1}{m} \frac{\partial U(x, z)}{\partial x} = 0, \tag{7}$$

$$\ddot{z} + \frac{1}{m} \frac{\partial U(x, z)}{\partial z} = 0. \tag{8}$$

Using the conservation of energy, we can combine these two equations, eliminating time as variable, to generate a single equation governing $x$ as a function of $z$ (Ref. 3):

$$\frac{d}{dz}\left[\left(1 - \frac{U(x, z)}{E_0}\right)^{1/2} (1 + x'^2)^{-1/2} x'\right] + \frac{1}{2E_0}\left(1 - \frac{U(x, z)}{E_0}\right)^{-1/2} (1 + x'^2)^{1/2} \frac{\partial U(x, z)}{\partial x} = 0, \tag{9}$$

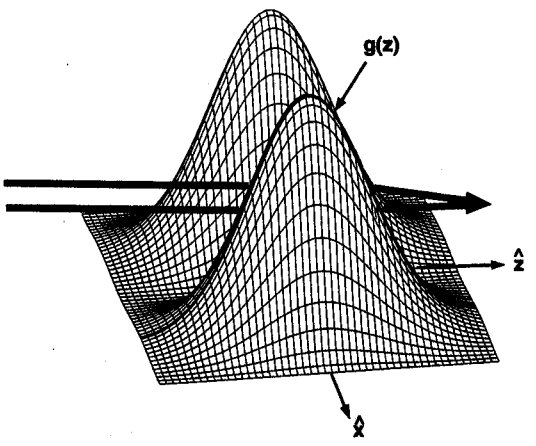


Fig. 1. Laser focusing of atoms in a standing wave, showing the sinusoidal behavior of the intensity along $\hat{x}$ and the envelope function $g(z)$ along $\hat{z}$. Note the difference in scales of the $x$ and $z$ axes; the periodicity along $x$ is typically hundreds of nanometers, while the envelope typically varies over hundreds of micrometers along $\hat{z}$.

where $E_0$ is the total energy of the atom (i.e., the kinetic energy in a field-free region) and $x'$ denotes differentiation of $x$ with respect to $z$. The application of particle optics to atom focusing in a standing wave is now reduced to solving Eq. (9) by use of the potential given by Eq. (2).

## 4. PARAXIAL SOLUTION

Equation (9) can be solved numerically to obtain an exact solution of the equation of motion. This will be considered in a subsequent section. To exploit fully the concepts of geometrical optics, however, it is valuable to consider first a paraxial solution, in which trajectories are assumed to be nearly parallel to the $\hat{z}$ axis. Focal lengths and principal plane locations can be derived, which are useful in determining the gross focal properties of the lens. The exact numerical solution can then be applied to check the range of validity of the paraxial solution and examine aberrations.

To make the paraxial approximation, we consider the focal properties of a single node of the standing wave (assuming $\Delta > 0$) and require that $U(x, z) \ll E_0$, $x' \ll 1$, and $kx \ll 1$. In this limit, Eq. (9), with $U(x, z)$ from Eq. (2) substituted, becomes

$$x'' + q^2 g(z) x = 0, \tag{10}$$

where

$$q^2 \equiv \frac{\hbar\Delta}{2E_0} p_0 k^2. \tag{11}$$

It is interesting to note that the requirements $kx \ll 1$ and $U(x, z) \ll E_0$ ensure that the laser intensity is low for paraxial trajectories, so in this limit one needs to worry less about saturation effects. We now consider solutions to Eq. (10) in a number of special cases.

### A. Constant Intensity

This situation is not particularly realistic because the atoms must enter the laser beam at some point, and the entry is not likely to be instantaneous. Nevertheless, it is useful to consider because it is the simplest case.

When $g(z) = 1$, the solution to Eq. (10) becomes

$$x(z) = A \sin qz + B \cos qz, \tag{12}$$

where $A$ and $B$ are constants chosen according to the initial conditions of the trajectory. We note that this solution is completely equivalent to the harmonic oscillator solution obtained in Ref. 8. To obtain the focal properties, we consider a trajectory initially parallel to the $z$ axis with $x = x_0$. We assume that the laser field starts instantaneously at $z = 0$. The evolution of the trajectory is then given by

$$x(z) = x_0 \cos qz. \tag{13}$$

This trajectory crosses the $z$ axis at a focal location

$$z_f = \pi/2q. \tag{14}$$

Since the trajectory is clearly curved and the focus is within the region of laser intensity, the lens is a thick immersion lens, and we must obtain a principal-plane location to derive the focal length. The principal plane is located at that $z$ value where the tangent to the trajectory at $z = -\infty$ intersects the tangent to the trajectory at the focus, or

$$z_p = \frac{\pi - 2}{2q} \quad \text{(constant intensity)}. \tag{15}$$

The focal length $f$ is found by determination of the distance between the principal plane and the focus, which gives the simple result

$$f = q^{-1} \quad \text{(constant intensity)}. \tag{16}$$

### B. Gaussian Beam Envelope

Since laser beams are generally Gaussian in profile, or at least approximately so, it is most useful to consider the case in which $g(z) = \exp(-2z^2/\sigma_z^2)$. Here $\sigma_z$ is the $1/e^2$ radius of the Gaussian laser beam. Unfortunately, the paraxial equation (10) cannot be solved analytically with this $g(z)$. Nevertheless, the trajectories of the atoms and hence the focal properties of the lens can be parameterized relatively simply either through approximation or a simple numerical calculation. We begin by converting the equation of motion to a form in which $z$ is replaced by a dimensionless quantity $Z \equiv z/\sigma_z$. The paraxial equation then becomes

$$x'' + a \exp(-2Z^2) x = 0, \tag{17}$$

where we have introduced the new parameter

$$a \equiv \sigma_z^2 q^2 = \frac{\hbar\Delta}{2E_0} p_0 k^2 \sigma_z^2. \tag{18}$$

First we consider the thin-lens approximation, which is valid for very weak focusing, i.e., when $a \ll 1$ and the focal length $f \gg \sigma_z$. In this case the asymptotic trajectories at $Z = \pm\infty$ are straight lines given by $x(-\infty) = A_1 + B_1 Z$ and $x(+\infty) = A_2 + B_2 Z$, with $A_1$, $B_1$, $A_2$, and $B_2$ constant. The action of the lens can be characterized by a ray transfer matrix $\mathbf{M}$:

$$\mathbf{M}\begin{bmatrix} A_1 \\ B_1 \end{bmatrix} = \begin{bmatrix} A_2 \\ B_2 \end{bmatrix}. \tag{19}$$

To solve for $\mathbf{M}$, a perturbation expansion in $a$ can be carried out,[12] and the result is

$$\mathbf{M} = \begin{bmatrix} 1 & a\left(\frac{\pi}{32}\right)^{1/2} \\ -a\left(\frac{\pi}{2}\right)^{1/2} & 1 \end{bmatrix}. \tag{20}$$

To obtain the focal length of the lens, we consider the behavior of a ray that is initially parallel to the axis, described by setting $B_1 = 0$. The ray into which this transforms, after passing through the lens, crosses the axis at the focal point. Using Eq. (20) to obtain $A_2$ and $B_2$ and finding the $z$ intercept of the trajectory, we obtain

$$F \equiv f/\sigma_z = \sqrt{2/\pi}\, a^{-1} \quad \text{(thin lens)}. \tag{21}$$

We note that, since the lens is thin in this approximation, the principal plane is always located at $z = 0$, i.e., at the center of the Gaussian laser beam.

The thin-lens approximation is useful in situations in which the standing-wave laser beam focuses the atoms at a point well outside the region of light intensity. However, this is generally the case of a weak lens, and the focal size will not be small. Much smaller foci are obtained when the focal length of the lens is much shorter. This occurs when the focal plane is within the laser beam itself, i.e., when the lens is a thick immersion lens. The thin-lens approach is no longer valid, and a numerical solution to Eq. (17) must be obtained. Because of the dimensionless parameterization of the lens in terms of $a$, though, the equation need only be solved once, and the results can be applied to any atom-focusing situation.

We have solved Eq. (17) numerically with initial conditions of a ray parallel to the $z$ axis to obtain the focal properties. The results are shown in Fig. 2, in which the scaled focal length $F$ and the principal-plane location $Z_p$ are plotted as a function of the excitation parameter $a$. This single universal plot is applicable to any standing-wave Gaussian-beam atom-focusing situation. To make use of it, one need only calculate $a$ from Eq. (18) and then read off the focal properties in units of the $1/e^2$ radius $\sigma_z$ of the Gaussian laser beam.

By examining Fig. 2 we can observe some instructive qualitative properties of the Gaussian standing-wave lens. For instance, if the goal is to make a shorter focal length, it is clear that it is not worth increasing $a$ (by, for example, increasing the laser power or decreasing the detuning) above a value of approximately 5. Beyond this value the principal-plane location moves out of the lens almost as much as the focus moves in, resulting in a slowly decreasing focal length. Also, if it is desired to focus the atoms at the center of the Gaussian laser beam, one must choose the value for $a$ at which $F = -Z_p$, i.e., $a = 5.37$ (determined numerically). This focal location has some practical interest because it permits an experiment to be aligned on the basis of symmetry.[7]

We can see further interesting properties of the lens by noting that $a$ is proportional to the laser intensity $I_0$ and the square of the $1/e^2$ radius $\sigma_z$. For a standing-wave Gaussian beam, $I_0$ is related to the incident traveling laser power $P_0$ by

$$I_0 = \frac{8P_0}{\pi {\sigma_z}^2}. \tag{22}$$

Thus when the focal properties of the lens are expressed in terms of the incident laser power, the dependence on ${\sigma_z}^2$ cancels, leaving $a$ independent of $\sigma_z$. As a result, the laser beam parameters that determine the essential behavior of the lens are only the power $P_0$ and the detuning $\Delta$. The beam radius $\sigma_z$ serves only as a scale-determining factor.

The scaling of the focal length with $\sigma_z$ permits one to fix the focal location at the center of the laser beam (a convenient configuration from a practical viewpoint) and still have a choice of focal lengths by choosing different laser beam sizes. The power required for bringing the lens into focus at the beam center is (for $\Delta \gg \gamma$)

$$P_{\text{focus}} = 5.37\,\frac{\pi E_0 I_s \Delta}{\hbar \gamma^2 k^2}. \tag{23}$$

As an example, consider a thermal Cr beam with $v = 926$ m/s, $\gamma = 3.15 \times 10^7$ rad/s, $I_s = 85$ W/m$^2$, $\lambda = 425.55$ nm (in vacuum), and $\Delta = 2\pi \times 200$ MHz. For these parameters, $P_{\text{focus}} = 2.9$ mW.

## 5. FOCAL LINEWIDTH AND ABERRATIONS

The focal properties described by Eqs. (15), (16), and (21), and Fig. 2 provide a basic description of laser focusing of atoms in a standing wave. However, since all of these results are derived from solutions of the paraxial equation, they necessarily represent approximations. Following the convention of particle optics, we group all behavior that is not covered by the paraxial equation into the category of aberrations.

Aberrations are of great interest because they determine the ultimate resolution of the standing-wave lens and hence determine how small a feature can be fabricated by use of laser focused deposition. Before considering aberrations, however, we discuss the contribution to the linewidth arising from the angular spread of the incident atom beam. This is not, strictly speaking, an aberration because it arises even in the paraxial approximation. Nevertheless, it is often the most significant contribution to the linewidth and hence needs to be estimated. Furthermore, it provides an illustration of the utility of the paraxial approximation.

Given the focal length of a lens, the contribution of the angular spread of an atom beam to the focal linewidth can be estimated by use of simple geometric optics. While a perfectly collimated atom beam will focus to an infinitesimally thin line at the focus of the lens, a nearly collimated beam, with angular divergence $\theta$, will focus to a small but finite line a short distance past the focus. To estimate the width of this line, we can represent the nearly collimated atom beam as arising from a virtual object at a position $-z_s$ with size $z_s\theta$, with $z_s \to \infty$. The image of this object will be nearly at the focus, demagnified by an amount $f/z_s$. The resulting linewidth is

$$s = f\theta. \tag{24}$$

This result can be used to generate a quick rough estimate of the contribution of atom beam collimation. For example, if the atoms are focused within the laser beam, Fig. 2 shows that the focal length will be of the order of

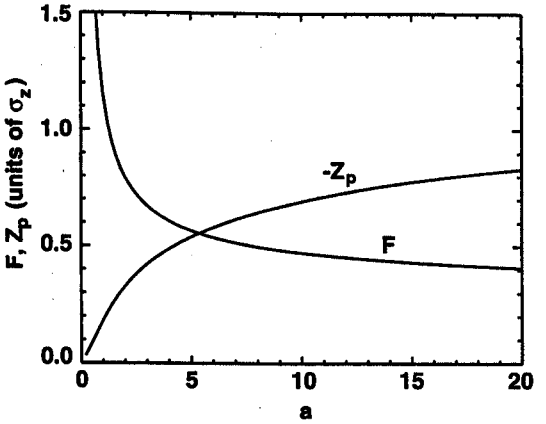


Fig. 2. Focal length $F$ and principal-plane location $Z_p$ for laser focusing of atoms in a standing wave with a Gaussian envelope versus the excitation parameter $a = p_0 k^2 {\sigma_z}^2 \hbar\Delta/(2E_0)$. $F$ and $Z_p$ are expressed in units of the $1/e^2$ radius $\sigma_z$ of the laser beam.

the Gaussian-beam $1/e^2$ radius $\sigma_z$. Considering the case of Ref. 7, we let $\sigma_z = 0.2$ mm and $\theta = 0.2$ mrad. The resulting linewidth estimate is 40 nm, not far from the measured value of 65 ± 6 nm.

### A. Diffraction

Diffraction, as an aberration, arises from the de Broglie wavelength of the atom and is completely neglected in any particle optics approach. Nevertheless, its effects on the linewidth can be estimated based on the focal length derived from the paraxial solution if we make the analogy to the diffraction limit of lenses in light optics. We restrict ourselves to considering cases in which the focal length is short enough so that contributions from neighboring potential wells in the standing wave do not overlap. For one-dimensional focusing the diffraction-limited full width at half-maximum is given by

$$d = 0.88 \frac{f \lambda_{dB}}{x_0}, \tag{25}$$

where $\lambda_{dB}$ is the de Broglie wavelength of the atom (based on its longitudinal momentum) and $x_0$ is the full width of the lens. While useful for rough estimates, this formula is somewhat difficult to apply precisely because $x_0$ is not well defined. Nevertheless, we can obtain a reasonable estimate by setting $x_0 = \lambda/2$. A full treatment of the effects of diffraction, especially in the presence of other aberrations, is beyond the scope of a particle optics approach and must be treated by means of a fully quantum approach such as a quantum Monte Carlo calculation.[13]

### B. Chromatic Aberration

The term chromatic aberration in a particle optics context is used to refer to the variation of focal length owing to particles passing through a lens with differing initial kinetic energies. The resulting range of focal lengths results in a blurring of the focus, limiting the resolution of the lens. Chromatic aberration can be a significant effect in the case of atom optics, mainly because atom beams typically have very broad velocity spreads. For example, an unselected effusive atomic beam has $\delta v/v \sim 1$. Several steps can be taken to reduce an atomic beam's velocity spread, such as employing a velocity selector, using supersonic expansion, or applying some laser cooling techniques. But practically speaking it is not generally possible to reduce the spread below 0.1 or possibly 0.01 without a large loss of flux.

To account properly for chromatic aberration when the atomic source is effusive and unselected, the only approach is to employ exact ray tracing, as discussed below. When $\delta v/v \sim 0.1$ or less, though, it is reasonable to use a differential approach. We consider a parallel beam that is being focused by a lens with focal length $f$ and ask by how much a ray will miss the focus if the velocity is varied by an amount $\delta v$. Using geometrical considerations, we see that the trajectory error $\delta x$ is given by

$$\delta x = \phi \delta f, \tag{26}$$

where $\phi$ is the convergence angle of the ray at the focus and $\delta f$ is the variation in the focal length owing to the velocity variation. We can obtain the focal length variation by noting that $f$ is a function of $a$, which is a function of $v$ through its dependence on $E_0$:

$$\delta f = \frac{df}{dv} \delta v = \frac{da}{dv} \frac{df}{da} \delta v = -2a \frac{df}{da} \frac{\delta v}{v}. \tag{27}$$

The resulting trajectory error is

$$\delta x = -2\phi a \frac{df}{da} \frac{\delta v}{v}. \tag{28}$$

To evaluate Eq. (28) for the Gaussian standing-wave lens, either the derivative $df/da$ is obtained numerically (see Fig. 3) or the thin-lens version $df/da = -2\sqrt{2/\pi}\, a^{-2} \sigma_z$ can be used if appropriate. An estimate of the linewidth contribution owing to chromatic aberration then consists of estimating the angle $\phi$ and using Eq. (28). For many situations, one can reasonably approximate $\phi$ by taking the lens size divided by the focal length, i.e., $\lambda/(2f)$.

### C. Spherical Aberration

Spherical aberration is a result of the higher-order terms in the equation of motion that cause trajectories to deviate from the path predicted by the paraxial equation. For instance, in the paraxial approximation any ray traveling parallel to the $z$ axis will cross the axis at the focal point after being focused by the lens. But in the actual standing-wave potential, which has the dependence $\ln(1 + \text{const.} \times \sin^2 kx)$, rays that enter the lens far from the axis feel a weaker force than is necessary to bring them to a focus at the focal point. The result is a focus that is no longer infinitesimal, but blurred.

The traditional way to calculate the effects of spherical aberration[14] is to expand the equation of motion and solve it by treating the next higher-order terms as a perturbation to the paraxial equation. This approach works well in cases in which the paraxial equation can be solved analytically[3] but becomes less useful when the paraxial equation must be solved numerically. Furthermore, it is less appropriate in cases in which the lens is not limited by any aperture and trajectories can enter in any part of the potential, experiencing forces that are quite different from those assumed in the paraxial approximation. Because the Gaussian standing-wave lens is a situation in which both these problems arise, we choose not to attempt an expansion of the equation of motion. Instead we go directly to a numerical solution of the exact equation of motion, wherein the effects of spherical aberration

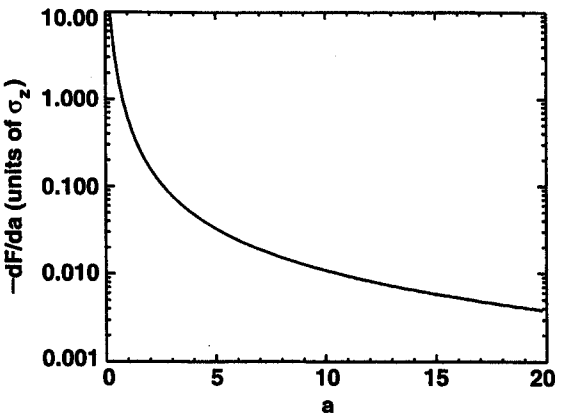


Fig. 3. Derivative of the focal length $F$ with respect to the excitation parameter $a$ for laser focusing of atoms in a standing wave with a Gaussian envelope. This is used to estimate chromatic aberration in the paraxial solution.

can be viewed explicitly. What is lost is a simple formula or two that can be used to predict approximate spherical aberration linewidths, but what is gained is a more exact and general solution. We hope that, by describing the method used to solve the equations of motion, it will appear simple enough for others to adapt to their own specific situations.

## 6. EXACT NUMERICAL SOLUTION

In this section we present a numerical solution for trajectories in the Gaussian standing-wave lens that does not rely on the paraxial approximation. This approach has its utility when the first-order properties have been observed and when it is desired to find out the effects of a very large velocity spread, large spherical aberration, or other higher-order effects.

We begin by noting that we must solve the second-order differential equation (9) for $x$ as a function of $z$ with Eq. (2) for the potential. From a numerical standpoint it is convenient to convert Eq. (9) into two coupled first-order differential equations in the variables $x$ and $\alpha \equiv x' = \mathrm{d}x/\mathrm{d}z$. Subsituting these variables, we obtain

$$x' = \alpha\,, \tag{29}$$

$$\alpha' = \frac{1+\alpha^2}{2(E_0 - U)}\left(\alpha\frac{\partial U}{\partial z} - \frac{\partial U}{\partial x}\right). \tag{30}$$

The solution of Eqs. (29) and (30) is readily obtained with any number of numerical packages. The potential $U(x, z)$ and its derivatives are simple analytic functions, so the solution is reasonably well behaved. We present here a few results calculated for the focusing of Cr atoms, for which $\lambda = 425.55$ nm (vacuum wavelength), $\gamma = 3.15 \times 10^7$ rad/s, $I_s = 85$ W/m$^2$, the atomic mass is 52 amu, and the most probable thermal velocity from a 1800-K oven is $v_0 = 926$ m/s.

Figure 4 shows the calculation of a series of trajectories, all initially parallel to the $z$ axis, entering the nodal region of a Gaussian standing wave at varying distances from the axis. The Gaussian standing wave was given a $1/e^2$ radius of 0.195 mm, corresponding to the experiment in Ref. 7. The laser detuning was 200 MHz, and the intensity was chosen to be $1.98 \times 10^5$ W/m$^2$, a value that results in $a = 5.37$, the condition required for focus at the center of the beam.

By inspection of Fig. 4 a comparison can be made with the paraxial solution, and the role of spherical aberration can be examined. As predicted by the paraxial solution, trajectories entering the lens close to the axis come to a focus at the center of the laser beam ($z = 0$). Trajectories entering farther away from the axis, on the other hand, miss the focal point because of spherical aberration. What is perhaps surprising is how small the effects of spherical aberration are, however. Also shown in Fig. 4 is the atomic flux at the focal plane, assuming a flux completely uniform in $x$ initially entering the lens. Despite the spherical aberration, the flux at the focal plane consists of a very narrow peak with a linewidth of only 1.0 nm. It appears that the major effect of spherical aberration is only to form a small pedestal around the foot of the focal peak.

While the spherical aberration of the lens shown in Fig. 4 is small, it is interesting to estimate the diffraction limit. Using Eq. (25) with $\lambda_{\mathrm{dB}} = 8.2$ pm, we obtain $d = 6.6$ nm, a value substantially larger than the spherical aberration linewidth. Thus in the absence of chromatic aberration and initial angular divergence the standing-wave lens is diffraction limited.

Figure 4 provides an illustration of the potential ultimate performance of a standing-wave lens, assuming no velocity or angular spread in the atom beam. However, it is of specific interest to examine the behavior of the lens when the incident atom beam contains a wide variety of initial velocities and angles. We can accomplish this by tracing a large number of trajectories, assigning a relative flux probability to each.

Figure (5a) shows such a calculation, in which initial conditions $(x_i, v_i, \alpha_i)$ for each trajectory were chosen on a grid, with $v_i$ used to set the initial kinetic energy $E_0$. Each trajectory was given a flux probability

$$P(x, v, \alpha)\mathrm{d}x\mathrm{d}v\mathrm{d}\alpha \propto v^4 \exp\left(-\frac{v^2}{2{v_0}^2}\right) \times \exp\left(-\frac{\alpha^2 v^2}{2{v_{0x}}^2}\right)\mathrm{d}x\mathrm{d}v\mathrm{d}\alpha\,, \tag{31}$$

and we determined the flux probability at the focal plane by creating a histogram, summing the probabilities of all trajectories that ended within a given $x$ bin after traversing the lens.

The probability relation (31) is independent of $x$ because the distribution in $x$ is uniform. We obtain the velocity and the angle dependence by taking the product of the thermal flux probability of having a longitudinal velocity $v$, proportional to $v^3 \exp(-v^2/2{v_0}^2)\mathrm{d}v$,

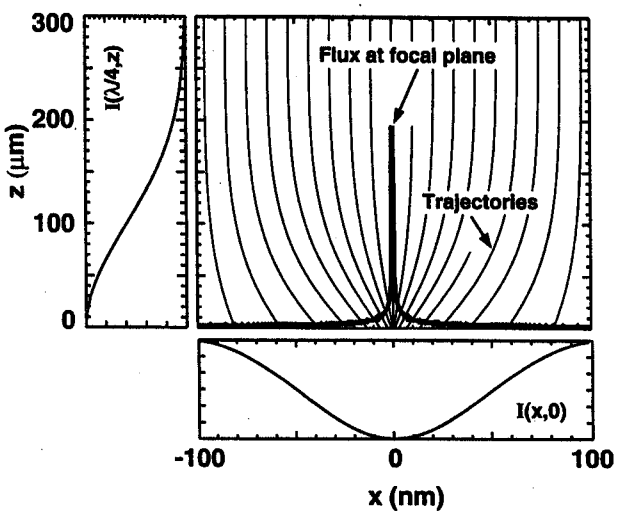


Fig. 4. Exact trajectory calculation of laser focusing of Cr atoms in a standing wave with a Gaussian envelope. A series of trajectories are shown for varying initial $x$ values. All trajectories are given the same initial velocity of 926 m/s and zero initial angle relative to the $z$ axis. Also shown is a plot of the atomic flux at the focal plane, assuming a uniform flux entering the lens, and laser beam profiles $I(x, z)$ along $\hat{x}$ (bottom) and $\hat{z}$ (left). For this calculation the $1/e^2$ radius was 195 $\mu$m, corresponding to the experiment in Ref. 3. The laser detuning was 200 MHz, and the intensity was chosen to be $1.98 \times 10^5$ W/m$^2$, a value that results in $a = 5.37$, the condition required for focus at the center of the laser beam.

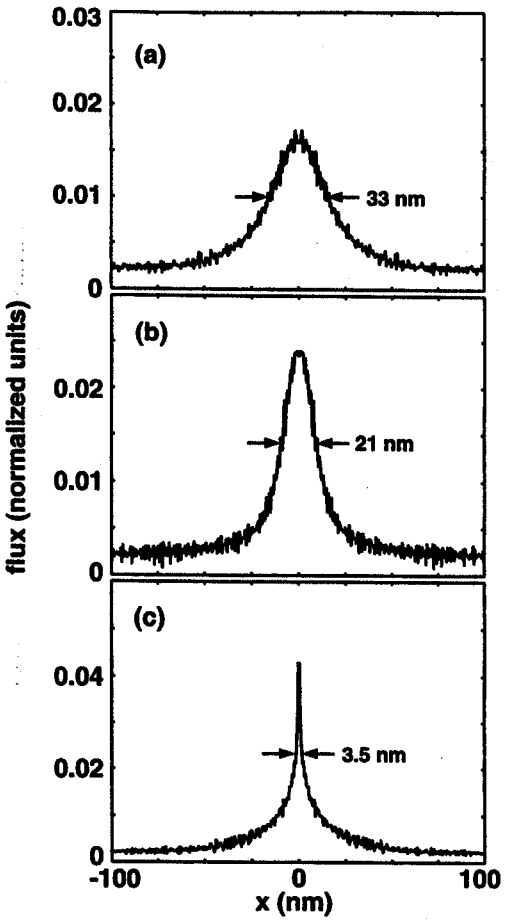


Fig. 5. Atomic flux distributions calculated by tracing trajectories through a standing-wave laser field with a Gaussian envelope. Laser and atomic beam parameters are the same as in Fig. 4 except as noted. The flux distributions are normalized such that the integral over $\lambda/2$ has the value of 1. (a) Atoms have a thermal longitudinal velocity distribution and an angular spread of $2 \times 10^{-4}$ rad (FWHM). (b) Atoms have a longitudinal velocity spread artificially narrowed to 1 m/s (FWHM) and an angular spread of $2 \times 10^{-4}$ rad (FWHM). (c) Atoms have a thermal longitudinal velocity spread and a narrowed angular spread of $1 \times 10^{-8}$ rad (FWHM).

and the probability of having a transverse velocity $v_x = \alpha v$, proportional to the Gaussian distribution $\exp(-v_x^2/2v_{0x}^2)dv_x$. The longitudinal velocity distribution is governed by the source temperature through $(1/2)k_B T_{\text{source}} = (1/2)mv_0^2$, and the transverse velocity spread is assumed to be generated by transverse laser cooling with rms velocity spread $v_{0x}$. It is assumed that the laser cooling has reached equilibrium, so that any correlations between $v_x$ and $v$ are nonexistent. Relation (31) can be written more simply as

$$P(v, \alpha) \propto v^4 \exp\left[-\frac{v^2}{2v_0^2}\left(1 + \frac{\alpha^2}{\alpha_0^2}\right)\right], \tag{32}$$

where we have introduced the quantity $\alpha_0 \equiv v_{0x}/v_0$. To apply relation (32), we obtain $v_0$ from the source temperature and derive $\alpha_0$ from a measurement of the degree of collimation produced by the laser cooling. The angle $\alpha_0$ is related to the FWHM of the angular distribution measured in a fluorescence experiment[15] by

$$\alpha_0 = \frac{\alpha_{\text{FWHM}}}{2\sqrt{\sqrt{2} - 1}}. \tag{33}$$

For the purpose of the calculation here the experimental value[7] $\alpha_{\text{FWHM}} = 0.2$ mrad was used.

Despite the broad velocity spread with $\delta v/v \sim 1$ present in a thermal atomic beam, the flux distribution shown in Fig. 5(a) still forms a peak at the focal point that has a surprisingly narrow FWHM of 33 nm. It is of interest to observe whether this width arises mostly from the velocity spread or the angular spread, or equally from both. To investigate this, we have recalculated the trajectories with an artificially narrowed velocity spread, shown in Fig. 5(b), and a narrower angular spread, shown in Fig. 5(c). The velocity spread was narrowed by replacement of the thermal flux distribution in relation (31) with a Gaussian centered at the most probable velocity $v_{\text{max}} = \sqrt{3}\,v_0$. We could vary the width of this Gaussian without changing the most probable velocity. Figure 5(b) was calculated with a FWHM of 1 m/s. We narrowed the angular spread for the calculation in Fig. 5(c) by reducing $\alpha_0$ to $1 \times 10^{-8}$.

Figure 5(b) shows the remarkable effect that, even when the width of the velocity distribution is drastically reduced, the linewidth at the focal plane is only reduced by 36%. Conversely, Fig. 5(c) shows that, even with a broad thermal velocity distribution, a narrow linewidth can be obtained, albeit with a broad pedestal. We note that the flux distribution shown in Fig. 5(c) is quite similar to what was obtained in Ref. 8 when a distribution in velocities was considered.

The conclusion that must be drawn from Fig. 5 is the somewhat counterintuitive one that the broad velocity spread in the atomic beam plays a much less significant role in determining the linewidth than does the degree of collimation of the incident atomic beam. We can shed some light on this apparent insensitivity to velocity spread by recognizing that all the atoms with velocities less than that of the most probable have focal points before the desired focal plane. Since the focal point is within the lens, these trajectories continue to be focused after crossing the axis and are effectively channeled through the lens; that is, they continue to be affected by a potential that becomes steeper and tighter because of increasing laser intensity, and their trajectories are kept near the axis. The trajectories with higher velocities are indeed focused less effectively, but the result is that they follow straighter paths, creating a more or less constant background.

## 7. CONCLUSION

In this paper we have constructed a framework that facilitates thinking about the focusing of atoms in a laser standing wave and in particular provides a series of simple formulas for making numerical estimates of the focal properties of the lens formed by each node of the standing wave. We have discussed a paraxial approximation that permits the application of a range of elementary geometric optics concepts to the lens, and then we have considered aberrations and a more exact numerical solution, with an emphasis on predicting linewidths at the focal plane.

The degree to which the ray-tracing approach discussed here can be used to accurately predict linewidths in a deposition process is an ongoing topic of research, and, as

more experiments are conducted, a better understanding of this will be forthcoming. Certainly there are a number of phenomena that are not considered in this model that might have some influence on the outcome. These range from fundamental considerations such as the applicability of the potential equation (2) in view of velocity-dependent forces, spontaneous emission, and dipole force fluctuations, to quantum considerations such as proper treatment of quantization of the translational motion of the atoms, to practical considerations such as surface diffusion and growth issues. Nevertheless, the framework presented here, because of its simplicity, should prove useful at least as a starting point for analyzing the behavior of an atomic lens formed by a near-resonant laser standing wave.

## ACKNOWLEDGMENTS

The author thanks Robert E. Scholten, Rajeev Gupta, and Robert J. Celotta for feedback and discussions regarding this study. Grateful acknowledgment is also extended to Mark Stiles and Charles W. Clark for theoretical guidance. This research is supported in part by the Technology Administration of the U.S. Department of Commerce and by the National Science Foundation under grant PHY-9312572.

## REFERENCES AND NOTES

1. V. I. Balykin and V. S. Letokhov, "The possibility of deep laser focusing of an atomic beam into the Å-region," Opt. Commun. **64,** 151–156 (1987).
2. G. M. Gallatin and P. L. Gould, "Laser focusing of atomic beams," J. Opt. Soc. Am. B **8,** 502–508 (1991).
3. J. J. McClelland and M. R. Scheinfein, "Laser focusing of atoms: a particle optics approach," J. Opt. Soc. Am. B **8,** 1974–1986 (1991).
4. C. S. Adams, M. Sigel, and J. Mlynek, "Atom optics," Phys. Rep. **240,** 143–210 (1994).
5. T. Sleator, T. Pfau, V. Balykin, and J. Mlynek, "Imaging and focusing of an atomic beam with a large period standing light wave," Appl. Phys. B **54,** 375–379 (1992).
6. G. Timp, R. E. Behringer, D. M. Tennant, J. E. Cunningham, M. Prentiss, and K. K. Berggren, "Using light as a lens for submicron, neutral-atom lithography," Phys. Rev. Lett. **69,** 1636–1639 (1992).
7. J. J. McClelland, R. E. Scholten, E. C. Palm, and R. J. Celotta, "Laser-focused atomic deposition," Science **262,** 877–880 (1993).
8. K. K. Berggren, M. Prentiss, G. L. Timp, and R. E. Behringer, "Calculation of atomic positions in nanometer-scale direct-write optical lithography with an optical standing wave," J. Opt. Soc. Am. B **11,** 1166–1176 (1994).
9. J. Dalibard and C. Cohen-Tannoudji, "Dressed-atom approach to atomic motion in laser light: the dipole force," J. Opt. Am. B **2,** 1707–1720 (1985).
10. See the feature issues on the mechanical effects of light, J. Opt. Soc. Am. B **2,** 1706–1860 (1985), and on laser cooling and trapping of atoms, J. Opt. Soc. Am. B **6,** 2020–2226 (1989).
11. J. P. Gordon and A. Ashkin, "Motion of atoms in a radiation trap," Phys. Rev. A **21,** 1606–1617 (1980).
12. C. W. Clark (National Institute of Standards and Technology, Gaithersburg, Md. 20899) contributed this derivation.
13. P. Marte, R. Dum, R. Taïeb, P. D. Lett, and P. Zoller, "Quantum wave function simulation of the resonance fluorescence spectrum from one-dimensional optical molasses," Phys. Rev. Lett. **71,** 1335–1338 (1993).
14. P. Grivet, *Electron Optics,* 2nd ed. (Pergamon, Oxford, 1972).
15. R. E. Scholten, R. Gupta, R. J. Celotta, and I are preparing a paper to be called "Laser cooling of a chromium beam."